

PS Static Reservoir Modeling of the Valanginian Depositional Sequence of Gamtoos Basin, Offshore South Africa*

Oluwatoyin L. Ayodele¹, Tapas K. Chatterjee¹, and J. M. van Bever Donker¹

Search and Discovery Article #11180 (2019)**

Posted January 14, 2019

*Adapted from poster presentation given at 2018 International Conference and Exhibition, Cape Town, South Africa, November 4-7, 2018

**Datapages © 2019 Serial rights given by author. For all other rights contact author directly. DOI:10.1306/11180Ayodele2019

¹Department of Earth Sciences, University of the Western Cape, Cape Town, South Africa (3217090@myuwc.ac.z)

Abstract

Gamtoos Basin is an echelon sub-basin under the Outeniqua offshore Basin near the South coast of South Africa. Gamtoos Basin is a complex rift type basin with onshore and offshore components, and consists of relatively simple half grabens bounded by a major fault to the northeast. The basin fill comprises organic-rich shale of considerable thickness that is considered responsible for generation of hydrocarbons in this area. This study is mainly focused on formation evaluation of the reservoir heterogeneity of the Valanginian depositional sequence. The prime objective of this work is to generate a 3D static reservoir model for better understanding of the spatial distribution of discrete and continuous reservoir properties (porosity, permeability and water saturation) of the depositional sequence. The methodology adopted in this work includes an integration of 2D-volume seismic data and well log data from six selected wells. These data were used to construct 3D-models of lithofacies, porosity, permeability and water saturation through petrophysical calculation, upscaling, Sequential Indicator Simulation (SIS) and Sequential Gaussian Simulation (SGS) algorithms, respectively. The statistical analysis model revealed that the effective porosity, permeability and water saturation concentration ranges between 8% to 19%, 0.1 mD (< 1.0 mD) to 1.0 mD, and 30% to 45% respectively across the study area from the north to the south in the basin. The result shows that the Valanginian depositional sequence is a potential hydrocarbon bearing reservoir revealed by the water saturation cut-off value, with good to poor porosity and poor permeability from the north to the southern part of the basin.

Static Reservoir Modeling of the Early Cretaceous Valanginian Depositional Sequence, Gamtoos Basin, Offshore South Africa.

Oluwatoyin L. Ayodele , Tapas K. Chatterjee , JM van Bever Donker.

Department of Earth Sciences, University of the Western Cape, Cape Town, South Africa.

Email:3217090@myuwc.ac.za



UNIVERSITY of the
WESTERN CAPE



Introduction

- An understanding of uncertainties entailed in reservoir modeling is a crucial tool to support decision making in the petroleum industry.
- The reservoir modeling is an effective technique that plays a major role in assisting reservoir managements for any decision relates with the development and reduction of hydrocarbon reserves, which must be taken into a consideration regards to the uncertainties of the formation involved. In this study, these concepts were applied within an exploration block located in the Gamtoos Basin, offshore South Africa, to contribute an understanding of the reservoir heterogeneity of the hydrocarbon exploration.
- The study focuses on formation evaluation of the reservoir heterogeneity using well log and 2D seismic data respectively.
- Objectively to generated 3D-dimentional static modeling reservoir technique for better insight of the spatial distribution of discrete and continuous reservoir properties of porosity, permeability and water saturation) of the six drilled wells Ha-N1, Ha-I1, Ha-G1, Ha-A1, Ha-K1 and Ha-B2, study from the north to the south in the early Cretaceous (Valanginian) depositional sequences of the basin, by using Petrel Software 2014© and IP "interactive Petrophysics software" work station respectively. Based on this presentation, three wells Ha-G1 Ha-B2, and Ha-K1 from the north to the south shall be focused respectively in the study area.

Study Location and Geology

The study area is within an exploration block in the Gamtoos Basin, Offshore South Africa.

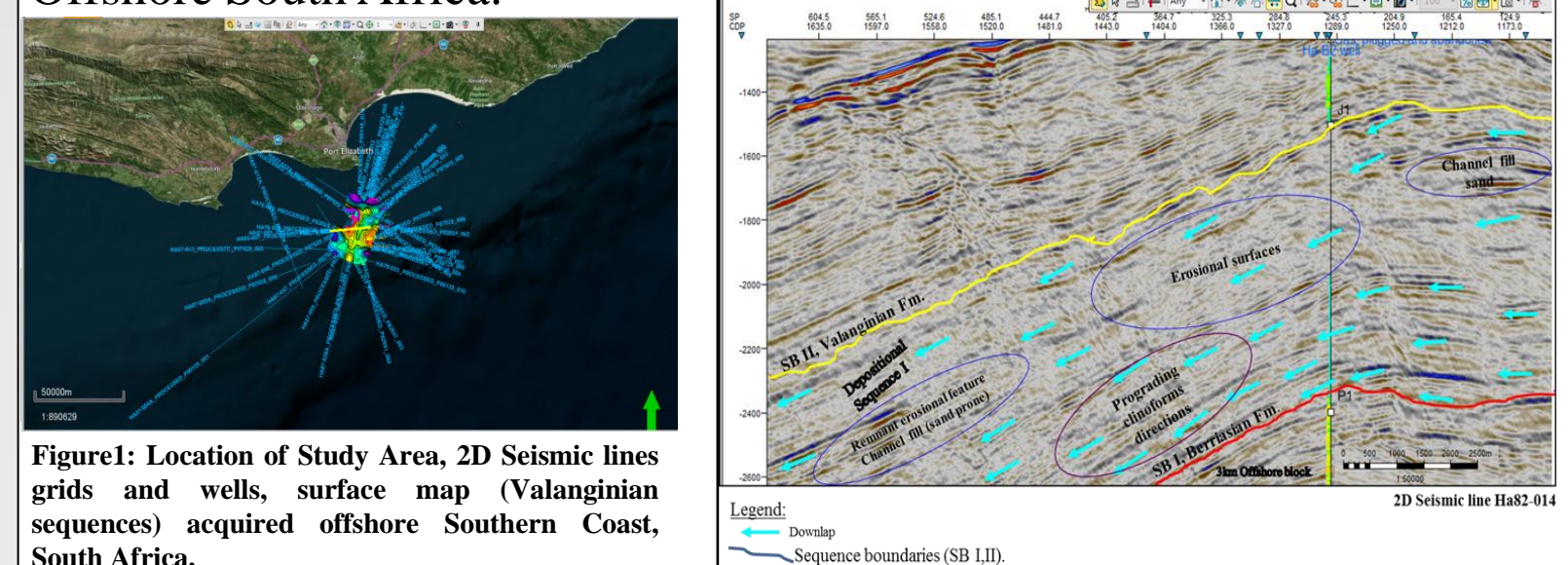


Figure 1: Location of Study Area, 2D Seismic lines grids and wells, surface map (Valanginian sequences) acquired offshore Southern Coast, South Africa.

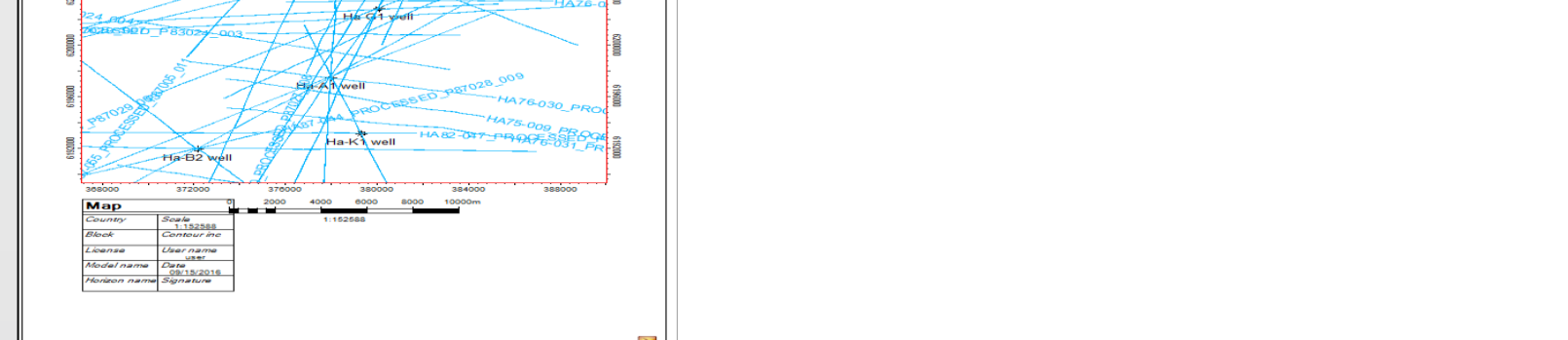
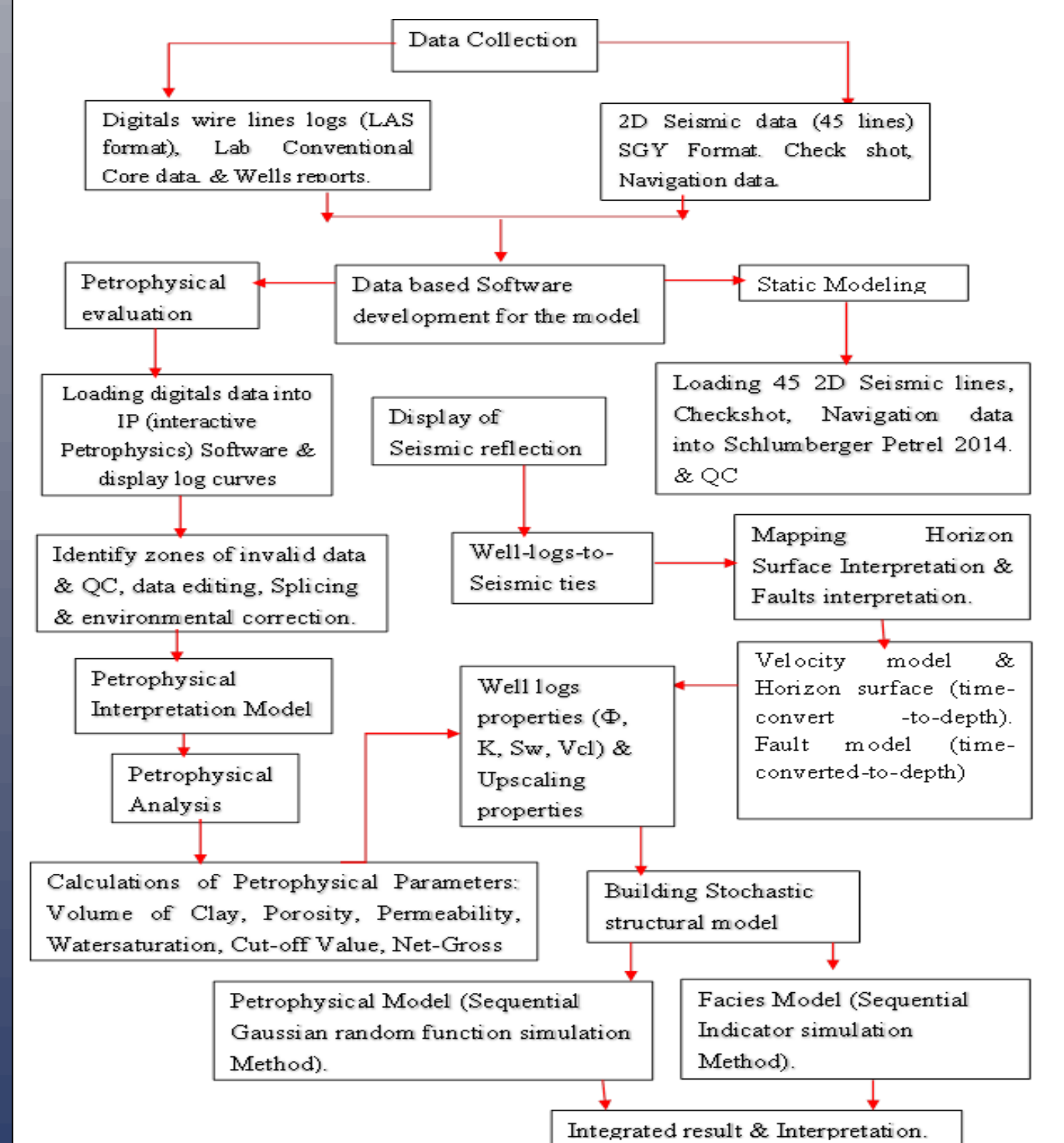


Figure 2: showing the map window processed 2D seismic line mapped horizon Valanginian sequence (Yellow line) a crossed the well utilized for the interpretation of the surface model for the study area.

- The Gamtoos Basin, located on the south-east margin of South Africa and extended from onshore areas to the offshore region, covers about 5,038 sq. km, attains a throw of 12km in the distal offshore, the eastern flank of the St. Francis arch along the Southern coast. It is a late Mesozoic basin which lies at the southernmost tip of the African plate (Malan, 1993).
- Its evolution occurred during the late Jurassic and earliest Cretaceous, but has been initiated in the Middle Jurassic (Malan, et al., 1990). The basin is structurally complex and severely faulted as a result of its proximity to the Agulhas-Falkland Fracture Zone (AFFZ) (Broad, 1990; Bate & Malan, 1992).
- It consists of relatively simple half grabens, bounded by a major fault to the northeast and containing comparable thicknesses of sediments. The oldest sediments encountered during the drilling dated to be Kimmeridgian (late Jurassic).
- The early and late rift subsidence sequences of these half grabens consist of thick sediments containing Kimmeridgian-to-Portlandian-to-Hauterivian (D to 6At1) wet gas to oil prone shale with sandstone reservoir potential in the Valanginian.
- In addition, the late rift subsidence during the Hauterivian also enabled deposition of thick sediments of organic-rich shale rock for petroleum generation (Malan, et al., 2009; McMillan, et al., 1997).

Methods



Interpretation & Results

THE PETROPHYSICAL PROPERTIES DETERMINATION

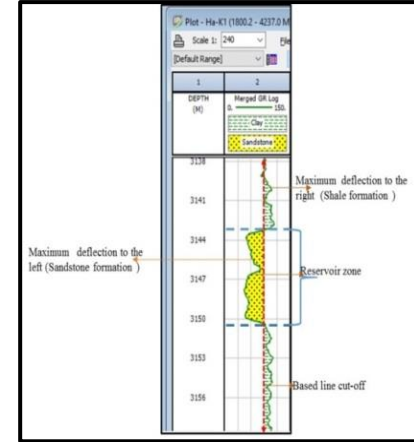


Figure 4: Illustrating an example of potential sandstone reservoir from one the well Ha-K1 study area.

THE POTENTIAL RESERVOIR ZONES OF THE SELECTED WELLS STUDY IN THE VALANGINIAN FORMATION.

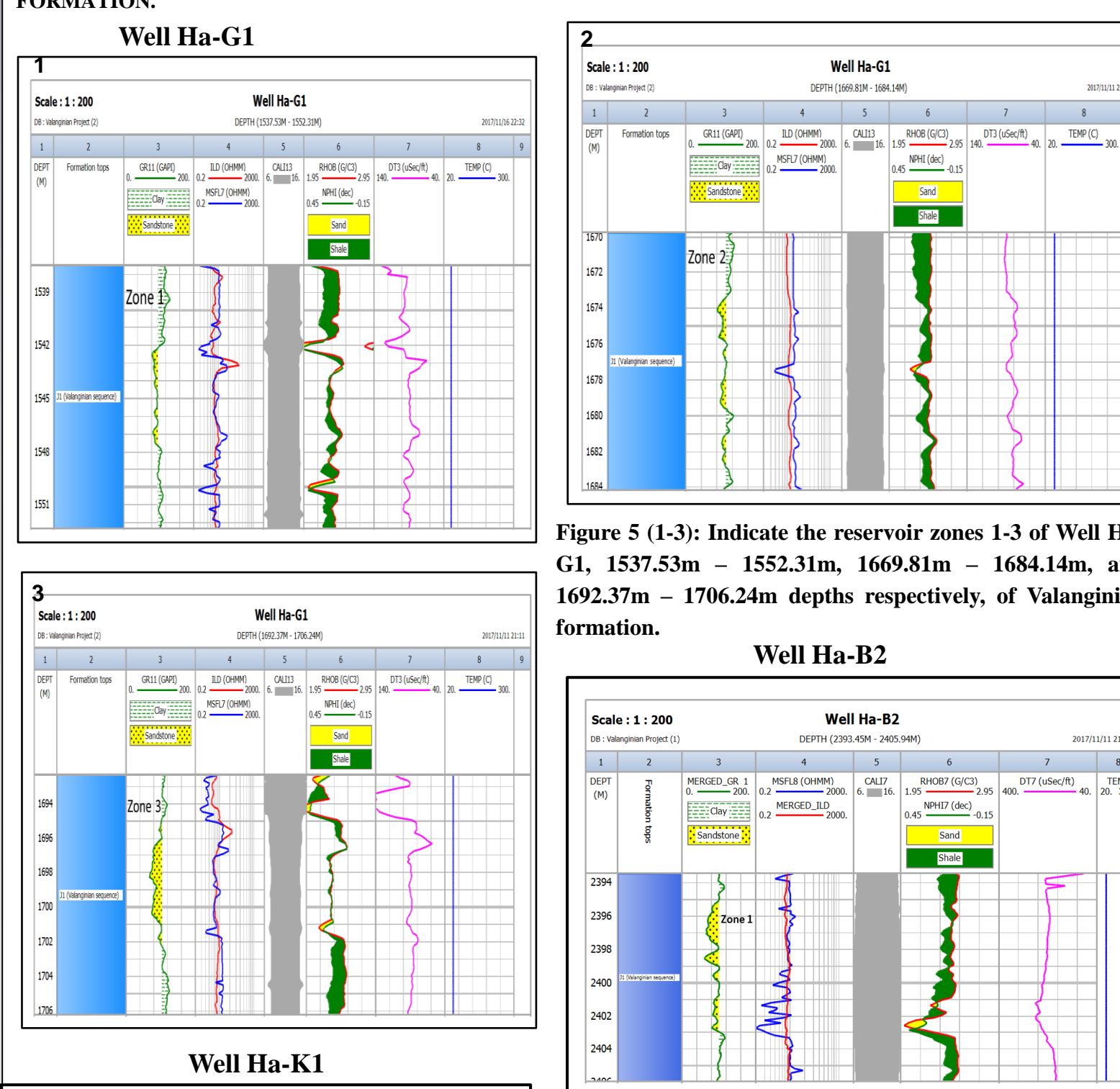


Figure 5 (1-3): Indicate the reservoir zones 1-3 of Well Ha-G1, 1537.53m - 1552.31m, 1669.81m - 1684.14m, and 1692.37m - 1706.24m depths respectively, of Valanginian formation.

Figure 6: Indicate reservoir zone well Ha-B2, 2393.45m - 2405.94 m depth of the Valanginian formation.

Figure 7: Indicate reservoir zone well Ha-K1, 3141.78m - 3151.99 m depth of the Valanginian formation.

THE INITIAL FLUID PARAMETER DETERMINATION IN THE FORMATION

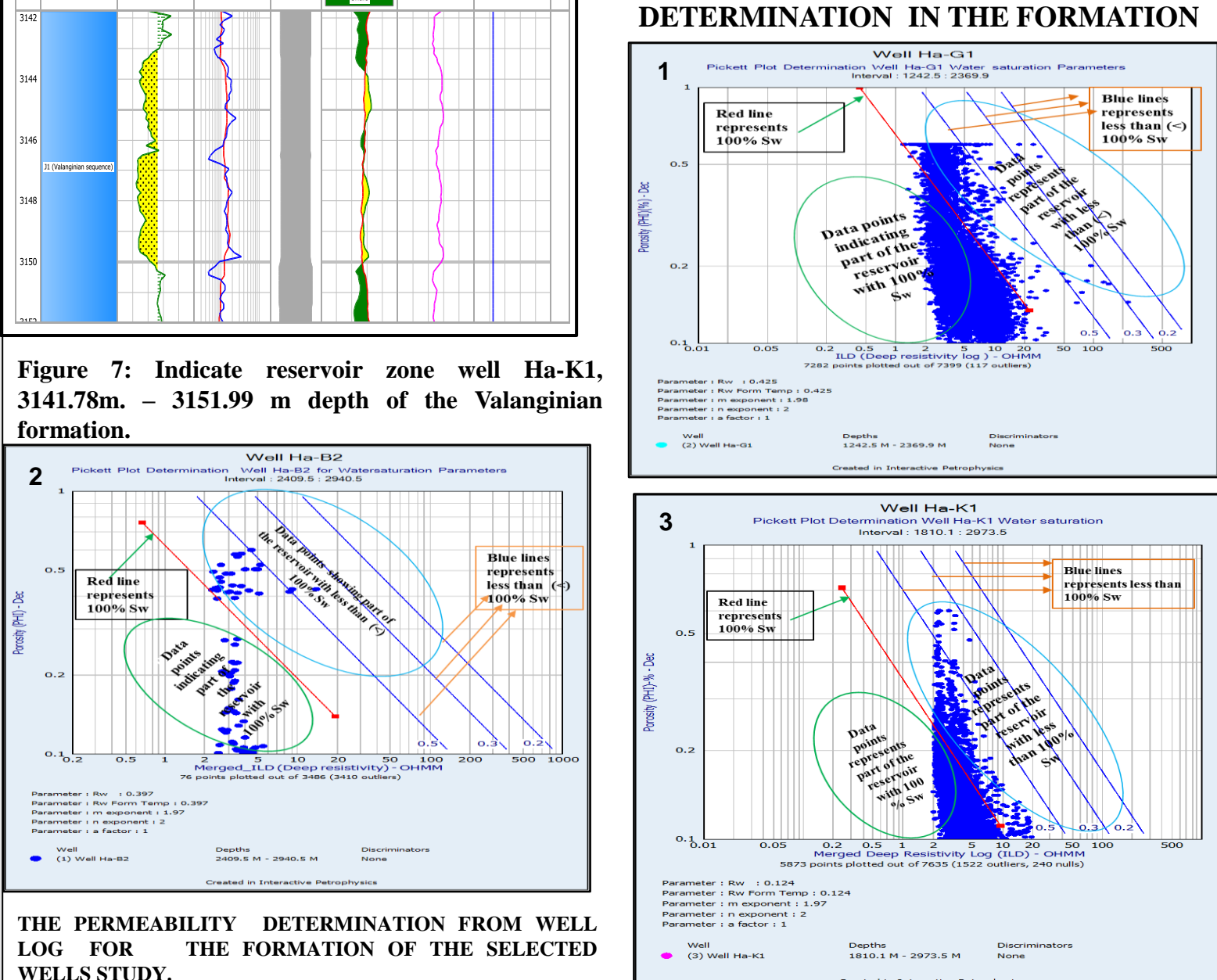


Figure 8 (1-3): Indicate the Pickett plot of Wells Ha-G1, Ha-B2, and Ha-K1, respectively for the fluids parameters of the formation.

Figure 9 (1-3): Indicate the Porosity versus Permeability (poro-perm) cross plot of well Ha-G1, Ha-B2 and Ha-K1 respectively and regression equations used to calculate the permeability of the formation.

Figure 10: a & b (1-3), indicating the calibrated models effective porosity and water saturation log curves with core data and the agreed best fits model log curves of wells, Ha-G1, Ha-B2,Ha-K1 respectively.

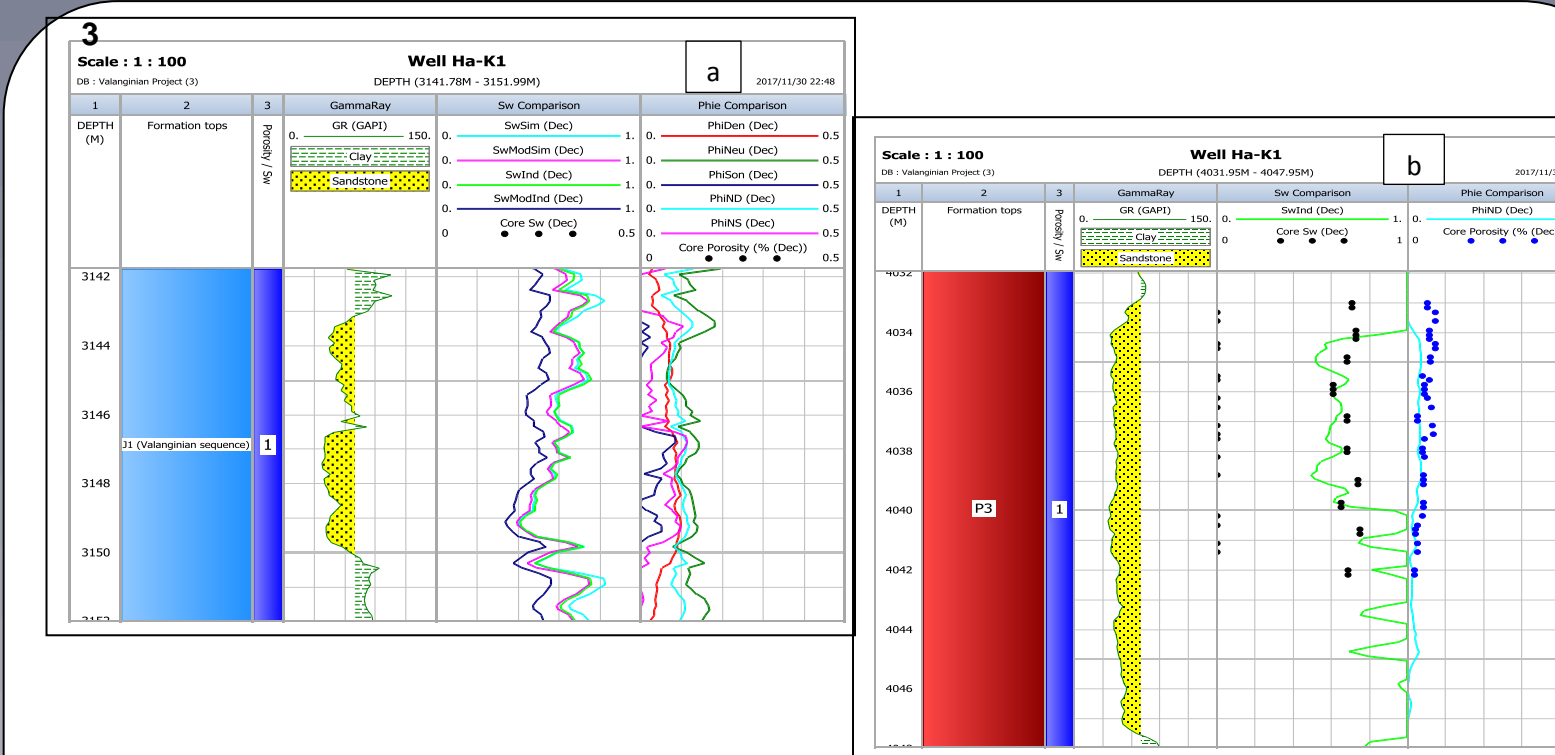


Figure 10: a & b (1-3), indicating the calibrated models effective porosity and water saturation log curves with core data and the agreed best fits model log curves of wells, Ha-G1, Ha-B2,Ha-K1 respectively.

THE CALCULATED PERMEABILITY K (mD) DETERMINATION FROM LOG FOR THE FORMATION FROM THE SELECTED WELLS Ha-G1, Ha-B2,Ha-K1.

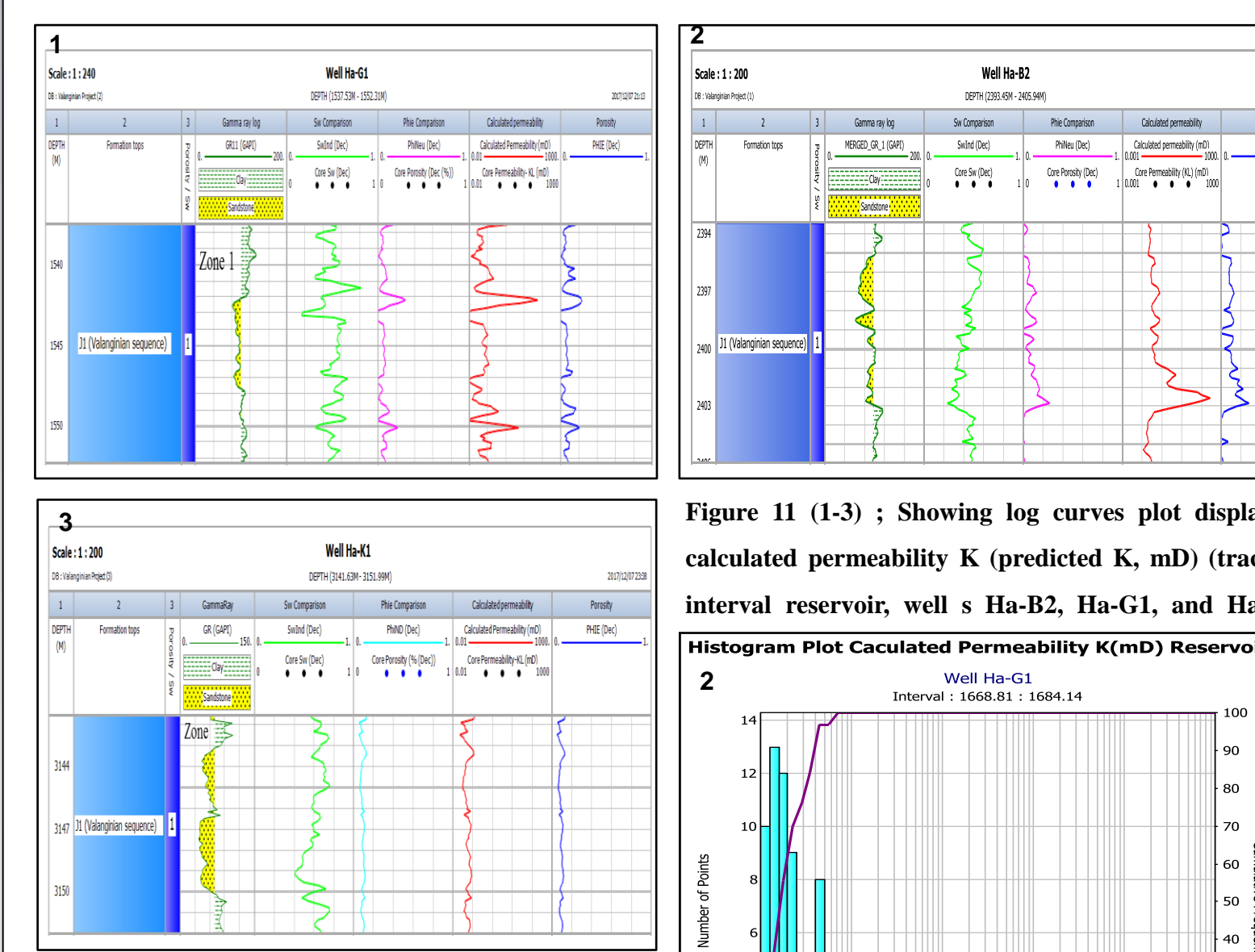


Figure 11 (1-3): Showing log curves plot displaying calculated permeability K (predicted K, mD) (track 7) interval reservoir, well s Ha-B2, Ha-G1, and Ha-K1.

Figure 12 (1-3): Histogram plot illustrating calculated permeability K (predicted K, mD) intervals reservoir of the selected wells Ha-B2, Ha-G1, Ha-K1, respectively.

THE POROSITY, PERMEABILITY & WATER SATURATION CUTOFF DETERMINATION FOR THE FORMATION FROM THE SELECTED WELLS Ha-G1, Ha-B2, & Ha-K1.

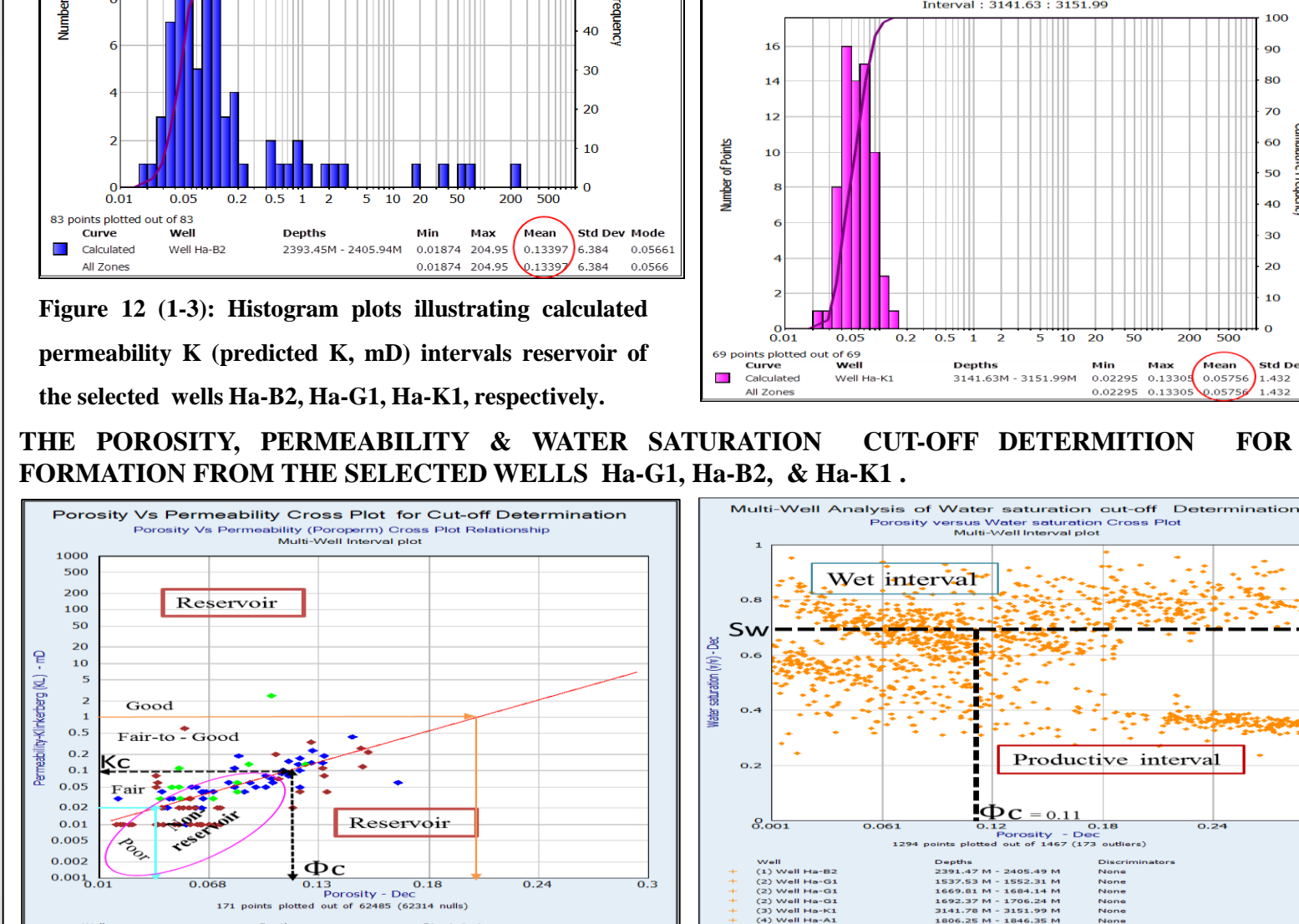


Figure 13: Illustrating the Porosity versus Permeability cross plot for cut-off determination.

Figure 14: Illustrating the cross plot cut-off determination for Multi-well Porosity against Watersaturation.

Figure 15: Illustrating the Core porosity histogram plot for the selected wells.

Figure 16: Illustrating the Core permeability histogram plot for the selected wells.

THE 3D RESERVOIR PROPERTY MODEL OF THE FORMATION

THE UPSCALING OF THE PARAMETERS WELL LOG POROSITY, PERMEABILITY AND WATERSATURATION

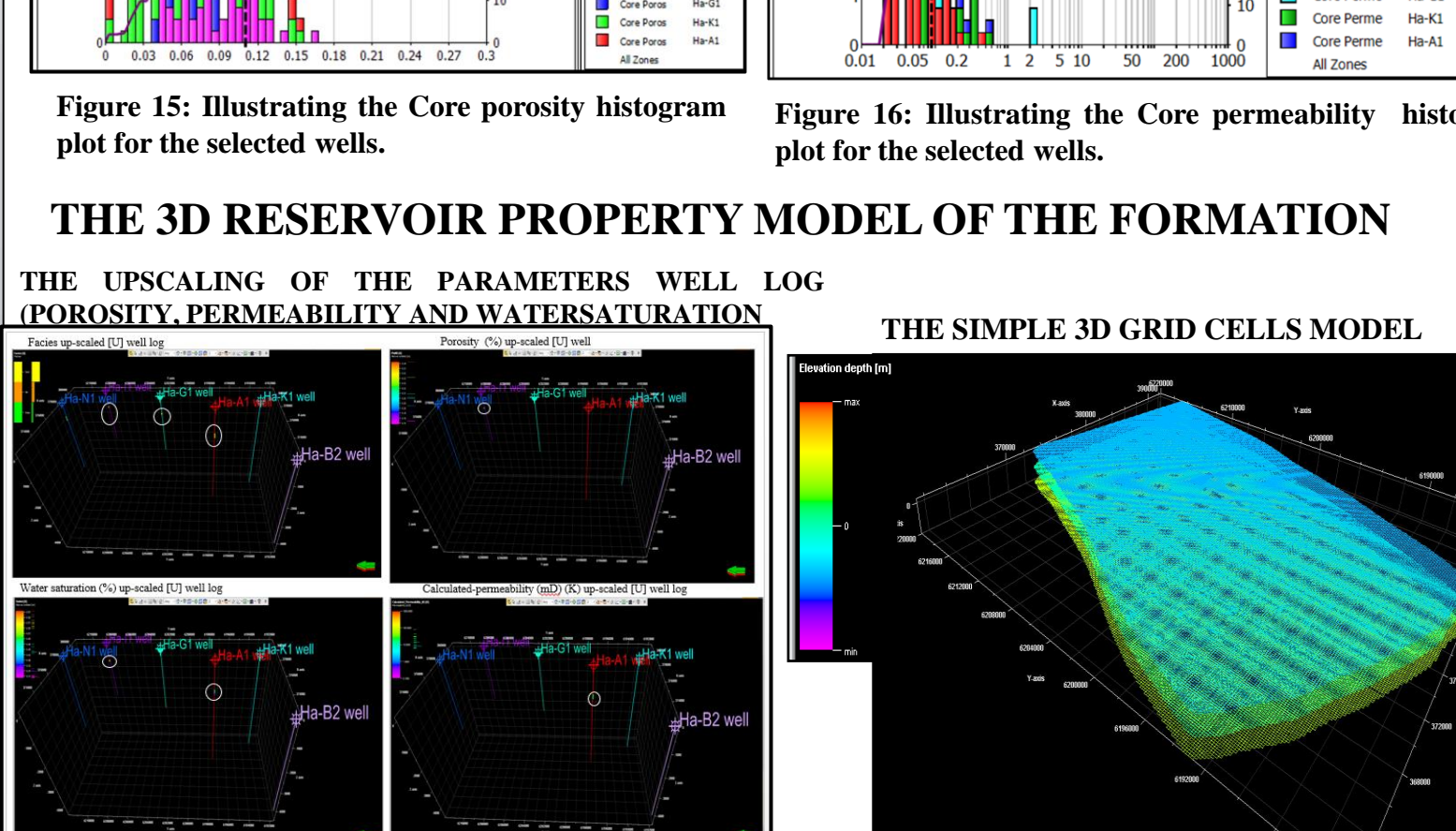


Figure 17: Dots in circles illustrating an Up-scaled [U] well logs parameters along the well path.

Figure 18: Showing the simple 3D cellular gridding cells (207 *238*21) area built through structural gridding.

Figure 19: Illustrating the 3D View of the time (ms) structured thickness map model of the Valanginian depositional sequence of the study area.

Figure 20: Illustrating the 3D View of the Depth (m) structured thickness map model of the Valanginian depositional sequence of the study area.

THE TIME(ms) STRUCTURE MAP SURFACE MODEL OF THE VALANGINIAN FORMATION.

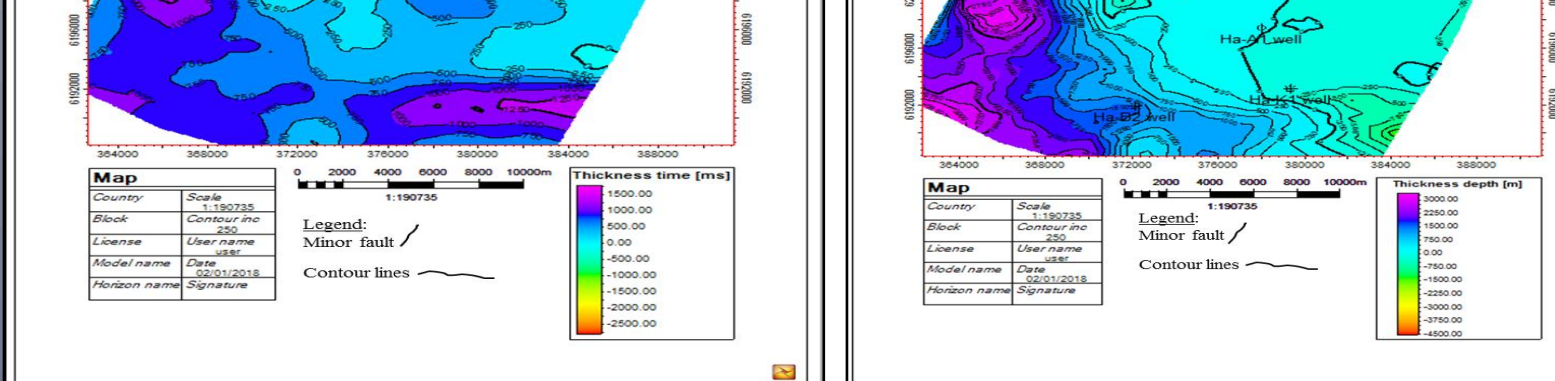


Figure 19: Illustrating the 3D View of the time (ms) structured thickness map model of the Valanginian depositional sequence of the study area.

THE DEPTH(m) STRUCTURE MAP SURFACE MODEL OF THE VALANGINIAN FORMATION.

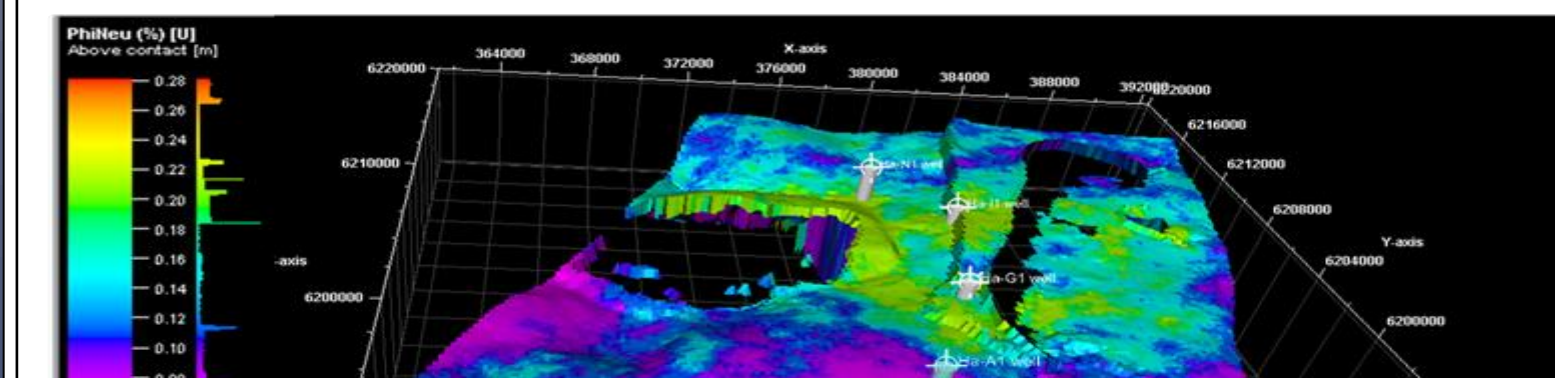


Figure 20: Illustrating the 3D View of the Depth (m) structured thickness map model of the Valanginian depositional sequence of the study area.

THE POROSITY MAP MODEL OF THE VALANGINIAN FORMATION.

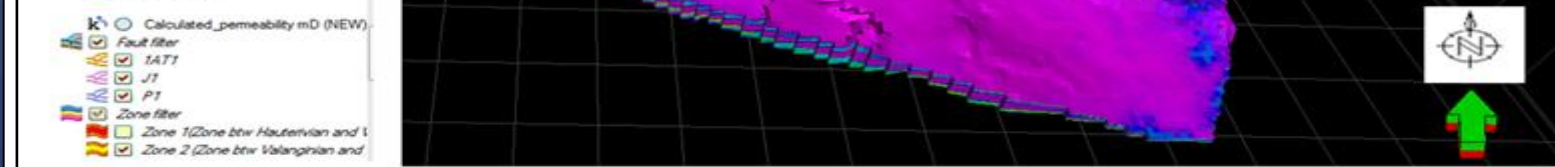


Figure 21: Illustrating the 3D View model of the Upscaled porosity model distributions across the Valanginian depositional sequence of the study area.

THE WATERSATURATION MAP MODEL OF THE VALANGINIAN FORMATION.

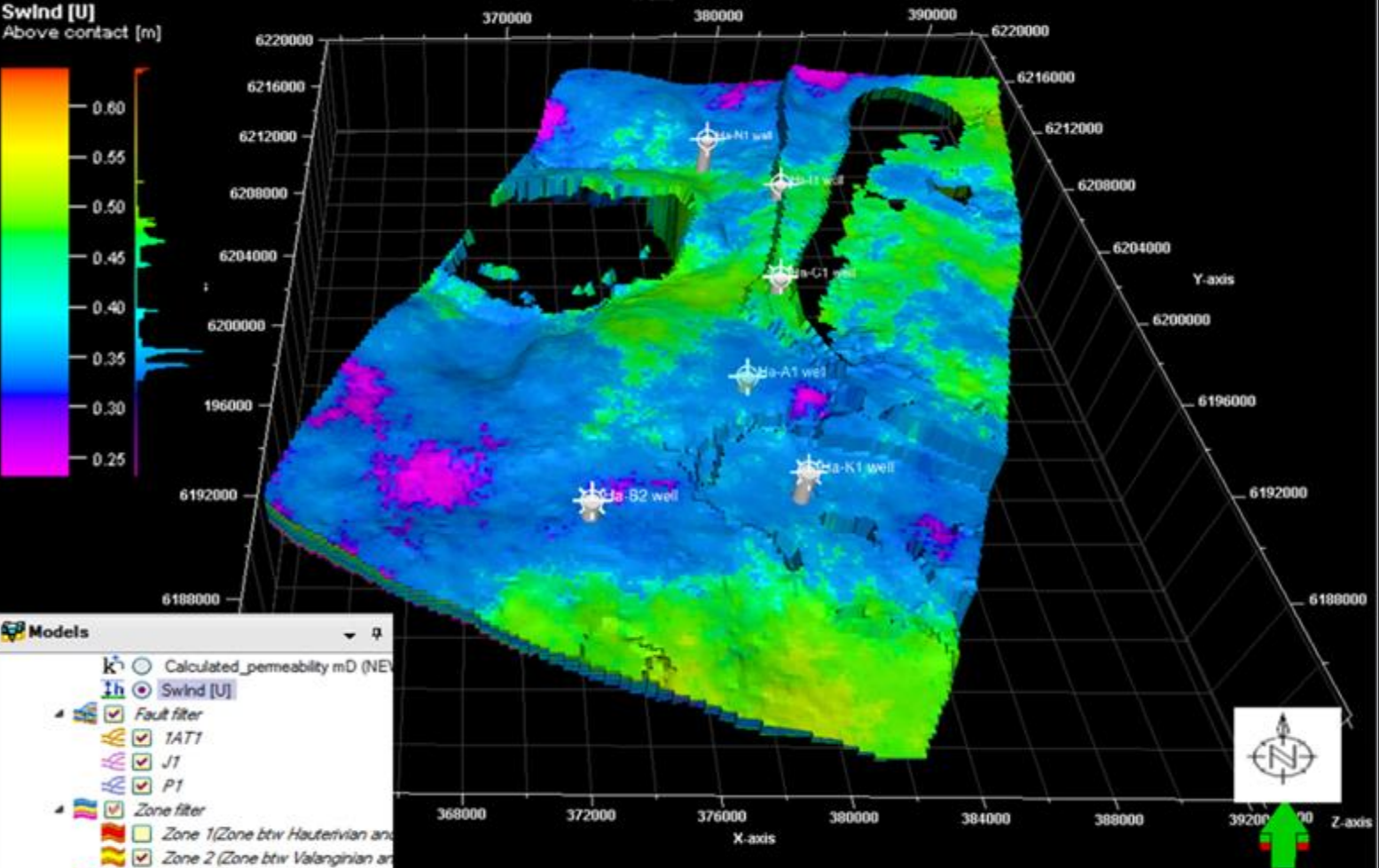


Figure 22: Illustrating the 3D View model of the Upscaled Watersaturation model distributions across the Valanginian depositional sequence of the study area.

THE PERMEABILITY MAP MODEL OF THE VALANGINIAN FORMATION.

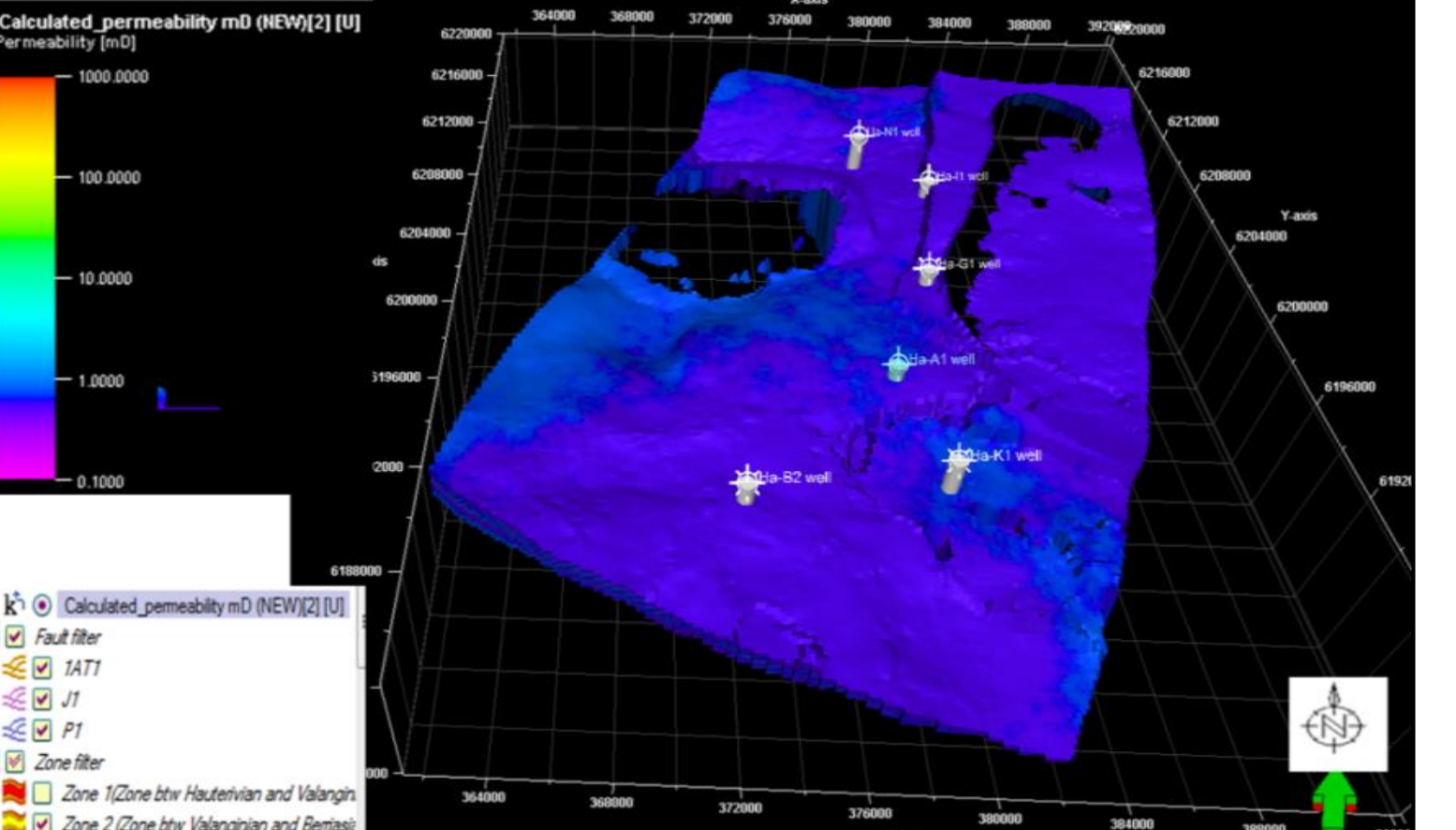


Figure 23: Illustrating the 3D View model of the Upscaled Permeability model distributions across the Valanginian depositional sequence of the study area.

THE LITHOFACIES MAP MODEL OF THE VALANGINIAN FORMATION.

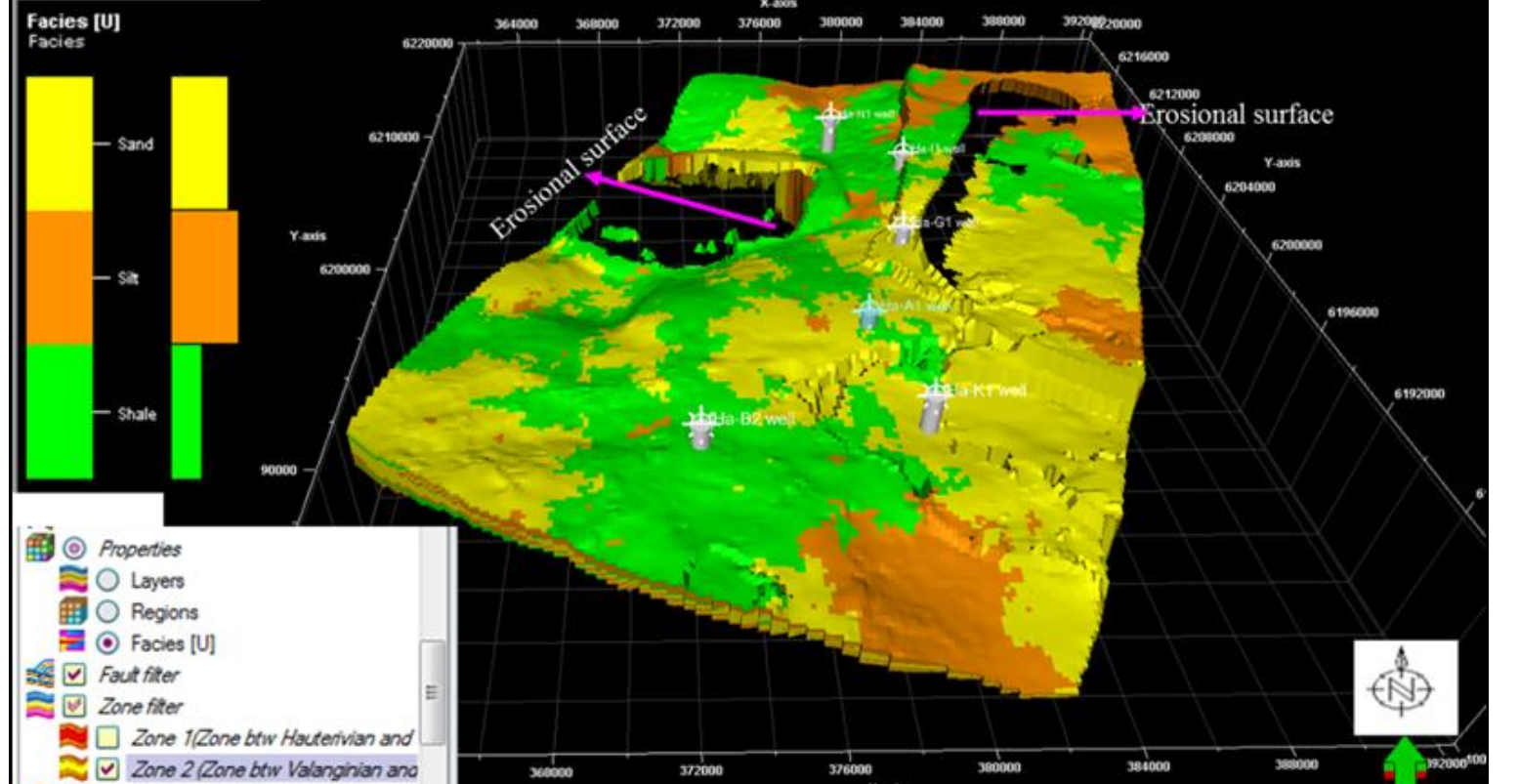


Figure 24: Illustrating the 3D View model of the Upscaled Lithofacies model distributions across the Valanginian depositional sequence of the study area.

Figure 25: Illustrating the 3D View model of the Upscaled Porosity model distributions across the Valanginian depositional sequence of the study area.

Figure 26: Illustrating the 3D View model of the Upscaled Permeability model distributions across the Valanginian depositional sequence of the study area.

Figure 27: Illustrating the 3D View model of the Upscaled Watersaturation model distributions across the Valanginian depositional sequence of the study area.

Figure 28: Illustrating the 3D View model of the Upscaled Lithofacies model distributions across the Valanginian depositional sequence of the study area.

Figure 29: Illustrating the 3D View model of the Upscaled Porosity model distributions across the Valanginian depositional sequence of the study area.

Figure 30: Illustrating the 3D View model of the Upscaled Permeability model distributions across the Valanginian depositional sequence of the study area.

Figure 31: Illustrating the 3D View model of the Upscaled Watersaturation model distributions across the Valanginian depositional sequence of the study area.

Figure 32: Illustrating the 3D View model of the Upscaled Lithofacies model distributions across the Valanginian depositional sequence of the study area.

Figure 33: Illustrating the 3D View model of the Upscaled Porosity model distributions across the Valanginian depositional sequence of the study area.

Figure 34: Illustrating the 3D View model of the Upscaled Permeability model distributions across the Valanginian depositional sequence of the study area.

Figure 35: Illustrating the 3D View model of the Upscaled Watersaturation model distributions across the Valanginian depositional sequence of the study area.

Figure 36: Illustrating the 3D View model of the Upscaled Lithofacies model distributions across the Valanginian depositional sequence of the study area.

Figure 37: Illustrating the 3D View model of the Upscaled Porosity model distributions across the Valanginian depositional sequence of the study area.

Figure 38: Illustrating the 3D View model of the Upscaled Permeability model distributions across the Valanginian depositional sequence of the study area.

Figure 39: Illustrating the 3D View model of the Upscaled Watersaturation model distributions across the Valanginian depositional sequence of the study area.

Figure 40: Illustrating the 3D View model of the Upscaled Lithofacies model distributions across the Valanginian depositional sequence of the study area.

Figure 41: Illustrating the 3D View model of the Upscaled Porosity model distributions across the Valanginian depositional sequence of the study area.

Figure 42: Illustrating the 3D View model of the Upscaled Permeability model distributions across the Valanginian depositional sequence of the study area.

Figure 43: Illustrating the 3D View model of the Upscaled Watersaturation model distributions across the Valanginian depositional sequence of the study area.

Figure 44: Illustrating the 3D View model of the Upscaled Lithofacies model distributions across the Valanginian depositional sequence of the study area.

Figure 45: Illustrating the 3D View model of the Upscaled Porosity model distributions across the Valanginian depositional sequence of the study area.

Figure 46: Illustrating the 3D View model of the Upscaled Permeability model distributions across the Valanginian depositional sequence of the study area.

Figure 47: Illustrating the 3D View model of the Upscaled Watersaturation model distributions across the Valanginian depositional sequence of the study area.

Figure 48: Illustrating the 3D View model of the Upscaled Lithofacies model distributions across the Valanginian depositional sequence of the study area.

Figure 49: Illustrating the 3D View model of the Upscaled Porosity model distributions across the Valanginian depositional sequence of the study area.

Figure 50: Illustrating the 3D View model of the Upscaled Permeability model distributions across the Valanginian depositional sequence of the study area.

Figure 51: Illustrating the 3D View model of the Upscaled Watersaturation model distributions across the Valanginian depositional sequence of the study area.

Figure 52: Illustrating the 3D View model of the Upscaled Lithofacies model distributions across the Valanginian depositional sequence of the study area.

Figure 53: Illustrating the 3D View model of the Upscaled Porosity model distributions across the Valanginian depositional sequence of the study area.

Figure 54: Illustrating the 3D View model of the Upscaled Permeability model distributions across the Valanginian depositional sequence of the study area.

Figure 55: Illustrating the 3D View model of the Upscaled Watersaturation model distributions across the Valanginian depositional sequence of the study area.

Figure 56: Illustrating the 3D View model of the Upscaled Lithofacies model distributions across the Valanginian depositional sequence of the study area.

Conclusions

- The 3D static reservoir model of the Valanginian formation depositional sequence of Gamtoos Basin, offshore South Africa has been studied for better understanding of the spatial distributions of discrete and continuous reservoir heterogeneity properties of the formation.
- By integrating of 2D-volume seismic data and petrophysical well log data from three selected wells, using Sequential Indicator Simulation (SIS) and Sequential Gaussian Simulation (SGS) algorithms model respectively.
- The statistical analysis model reveal the effective porosity, permeability and water saturation concentration ranges between 8% to 19%, 0.1mD (< 1.0 mD) to 1.0 mD and 30% to 45% respectively across the study area from the north to the south in the basin.
- The result shows that the Valanginian depositional sequence is a potential hydrocarbon bearing reservoir revealed by the water saturation cut-off value, with good to poor porosity and poor permeability from the north to the southern part of the basin.

References

- Abrahamsen, P., Omre, H. & Lia, O., 1991. *Stochastic Model for Seismic Depth conversions and Geological Horizons, Offshore Europe*, Aberdeen: Society of Petroleum Engineers (SPE 23138).
- Adotti, L. et al., 2014. Static Reservoir Modeling Using Well Log and 3-D Seismic Data in a KN Field, Offshore Niger Delta, Nigeria. *International Journal of Geosciences*, pp. 93 - 106.
- Bohling, G., 2005. *Stochastic Simulation and Reservoir Modeling Workflow In: Deutsch, C.V. 2002, Geostatistical Reservoir Modeling*. Kansas, Oxford University Press.
- Broad, D.S., 1990. Petroleum geology of Gamtoos and Algoa Basins. *Geological Society of South Africa*, PP 60 - 63.
- Lucia, F. J., 2007. *Carbonate Reservoir Characterization, An Integrated Approach*, Berlin: 2nd Edition, Springer.
- Malan, J. A., 1993. Geology, Potential of Algoa and Gamtoos Basin of South Africa. *Journal of Oil and Gas*, pp. 1 - 4.
- Worthington, P. F., 2008. *The application of cut-offs in Integrated reservoir studies*. Society of Petroleum Engineers (SPE) Reservoir Evaluation and Engineering (SPE 95428).
- Yu, X. & Li, X., 2012. *The Application of Sequential Indicator Simulation and Sequential Gaussian Simulation in Modeling a Case in Jilin Oilfield*, Qingdao, China: Exploration and Development Institute Jilin oilfield Company .